MAT JOURNALS

Journal of Recent Trends in Mechanics
Volume 4 Issue 1

The Effect of Changing the Slant Angle of Ahmed's Car Model on Drag Coefficient for Different Cruise Speeds

B. Zakher[1*], Dalia M. Ammar[2]
[1,2]Faculty, Department of Mechanical Engineering, Pharos University in Alexandria, Egypt
Email: **bassem.zakher1@gmail.com*

Abstract

The "Ahmed" body model is a model for a simplified car, consisting of a sharp nose with rounded edges fixed onto a two legs middle section and a rear end are slanted surface, the angle of which can be changed. The main aim of the present work is to study the effect of changing the slant angle on drag coefficient for constant Reynolds number and the effect of Reynolds number on drag coefficient for different slant angles

Keywords: *Velocity, Reynolds number, Aerospace sciences, Slant angle*

INTRODUCTION AND LITERATURE SURVEY

The Ahmed body gives all the features of flow around a car, flow impingement and displacement around the nose, relatively uniform flow around the middle and flow separation and wake generation at the rear [1].

Ahmed represented an experimental data which was obtained for a model length based Reynolds number of 4.29x106. He showed that the time averaged structure of the wake of a fast back type road vehicle housed a pair of a horseshoe vortices placed one above the other in the "separation bubble" emanating from vehicle base. He found the strength and location of the horse shoe vortices to be dependent upon the base start angle [2].

Cobalt, presented a study of parallel implicit, unstructured Euler/Navier Stokes flow solver to produce numerical results around Ahmed model. Many turbulence models including detached eddy simulation (DES) was used. This code is very useful for high Reynolds number, widely separated flows that is well known in aerodynamic engineering.

Ahmed and Morel, presented a 3-D external flow analysis on Ahmed reference model [3]. The aim of their study was to analyze the change in the drag coefficient with different rear slant angles. They concluded that pressure drag was the dominant component (85%) of the total drag acting on the car body and the rest of the drag was the friction drag [4]. The major part of the pressure drag was generated at the rear end (91%) and the frontal part was responsible for the rest of the drag. They showed that the pressure drag generated at the rear end depended very much on the rear slant angle [5]. They found that a critical slant angle of 30˚ existed above which a sudden drop in the drag coefficient occurred. For angles above the critical angle, contra-rotating vortices were found to be of less strength [6].

Gillieron and Chometon, presented numerical simulation using (k-□) model of version (4.2) of the fluent software and compared the results of the drag coefficient with the experimental results obtained by Ahmed et al. They also described the wake flow behavior for angles ranging between zero and lower critical angle along with these between lower critical angle and upper critical angle [7]. They also considered values above upper critical angle. From the results obtained on the simple shapes of Ahmed reference model, it would appear

viable to include computational methods in the analysis phases of a vehicle development cycle. This is because the friction for an Ahmed reference model is identical to those observed on an actual vehicle [8].

Howard et.al, presented large eddy simulation (LES) of an Ahmed reference model. The simulation was held for the case of 28˚ slant angle, which was very near to the critical angle (25 deg). The results was concluded for the time dependence of the drag coefficient and the flow behavior around the body.

INTRODUCTORY REMARKS ON AHMED BODY

The Ahmed model car is a simple geometric car body that retains the main flow features, specially the vortex wake flow where most part of the drag is. The "Ahmed" body, shown in Fig. 1, (like a "hatch-back" car) shows number of features of a real car (rotating wheels, rough underside, surface projections etc.).

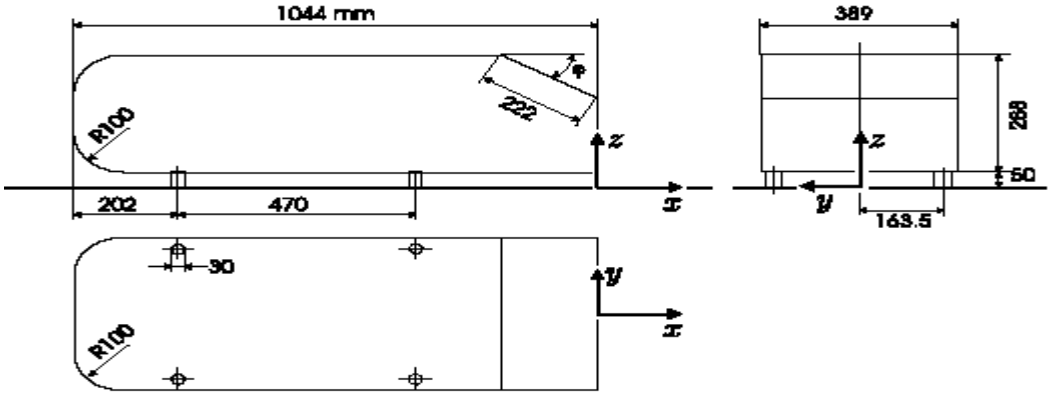

Figure 1: *Schematic of the Ahmed body model - dimensions in mm.*

DOMAIN AND MESH GRID DESCRIPTION FOR AHMED BODY

The Ahmed reference model is a generic car type bluff body shape which is enough simple for accurate flow simulation, but retains some important practical relevant features of automobile bodies. Details of structure layer for Ahmed body (slant angle 25 deg) are shown in Fig. 2. The total number of cells is 120127 cells [9]. The near-wall distribution of cells was arranged to maintain main-grid (y+) values of as many as possible near-wall cells around the body within the limits 30 < y+ < 300, but these limits were exceeded in some regions of stagnation and boundary-layer separation or reattachment [10].

According to linear k-ε model, the flow over the entire 25 degree rear slant was predicted to be fully attached with the coarse grid.

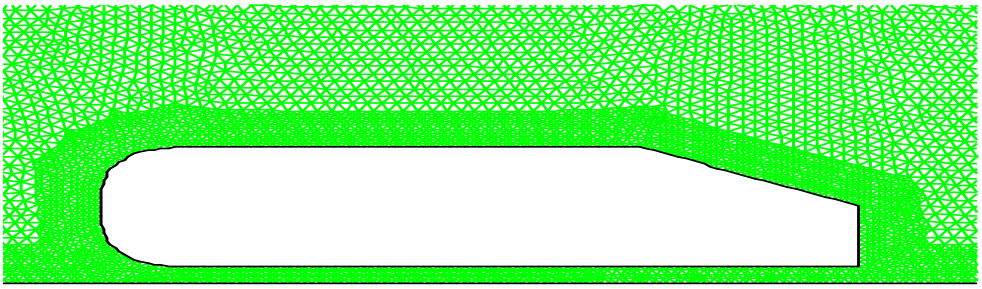

Figure 2: *Mesh grid for Ahmed body for 25 degree slant angle.*

GEOMETRY DESCRIPTION FOR AHMED BODY

Ahmed body is 1.044 m long, 0.288m high and 0.389m wide, area-0.112m^2, 0.05 m above ground, incoming flow velocity was made equal to 40m/s, corresponding to Mach number of 0.115, and incompressible air flow and no heat transfer are considered. The outflow is assumed fully developed, zero gradient velocity boundary condition is imposed and the ground and body surfaces are treated as no-slip smooth walls. Slant angles are in the range 25o $< \beta <$ 35^o .The drag coefficient C_D is calculated from,

$$CD = \frac{F_D}{0.5\rho u^2 A_X}$$

F_D: Total Drag Force (N)

ρ : Density (kg/m3)

U: Air flow velocity (m/s)

A_x: Projected area on X-Y axis for Ahmed body=0.288m2 (2-D)

Calculation of the drag coefficient

To study the drag coefficient for the present work, the drag is to be calculated from fluent results at different slant angles and one can get the total force acting on Ahmed body.

$$C_D = \frac{F_D}{282.24}$$ (for Ax=0.288 m2, u=40 m/s and ρ =1.225 kg/m3)

The Reynolds number here is defined as,

$$Re = \frac{\rho u l}{\mu}$$

For 40m/s air velocity, at constant air temperature

Re=2.859 ×106 (For μ=1.789x10-5 Pa s and l=1.044 m)

Using Reynolds number, the drag coefficient may be calculated from:

$$C_D = \frac{F_D (0.7148)^2 10^{10}}{0.1764(Re)^2}$$

$$C_D = (2.897 \times 10^{10}) \frac{F_D}{Re^2}$$

RESULTS AND DISCUSSION

The effect of changing the slant angle on drag coefficient for constant Reynolds number.

Figure 3 show the effect of slant angle on drag coefficient, for 0 deg slant angle. The coefficient of drag calculated from the results was (Cd = 0.602) which is a relatively high value. Two opposite vortices is appearing in the wake downstream of the body causing a region of separation due to lower pressure at its rear end as shown in Figure 4 by the velocity vectors for upstream velocity 40m/s (Re = 28.59 × 10^5).

As the slant angle is increased to 10 degree, the drag coefficient dropped to (Cd = 0.535) indicating that the rear slant has a great effect on the drag coefficient by decreasing the total force (pressure and viscous forces) acting on the body especially the pressure force. This can be seen from Fig. 5 where, the system of vortices generated behind the body close to the upper corner became weaker and evidently asymmetric.

For slant angle of 25 degree, it is found that the resulting pressure force and the viscous force decreased leading to a decrease in the total force giving a drag coefficient Cd=0.376 providing the optimum results obtained from Ahmed body design. This can be seen from Fig. 7 which shows the effect of 25 deg slant angle on the vortices generated at the rear end of Ahmed body. The extent of the system of vortices is greatly reduced.

As the slant angle is increased to 30 degree, we get a sudden rise in pressure force that takes place as the viscous force get a small change from (8.198 N) in 25 slant to (8.638 N) in 30° slant angle. This led to a sudden increase in the drag coefficient (Cd = 0.505).

It is clear from Fig. 8 that for 30 degree slant angle, the vortices generated at the

rear end of Ahmed body are very much influenced by the early flow separation that occurred at the rear end which has an adverse effect on the drag coefficient.

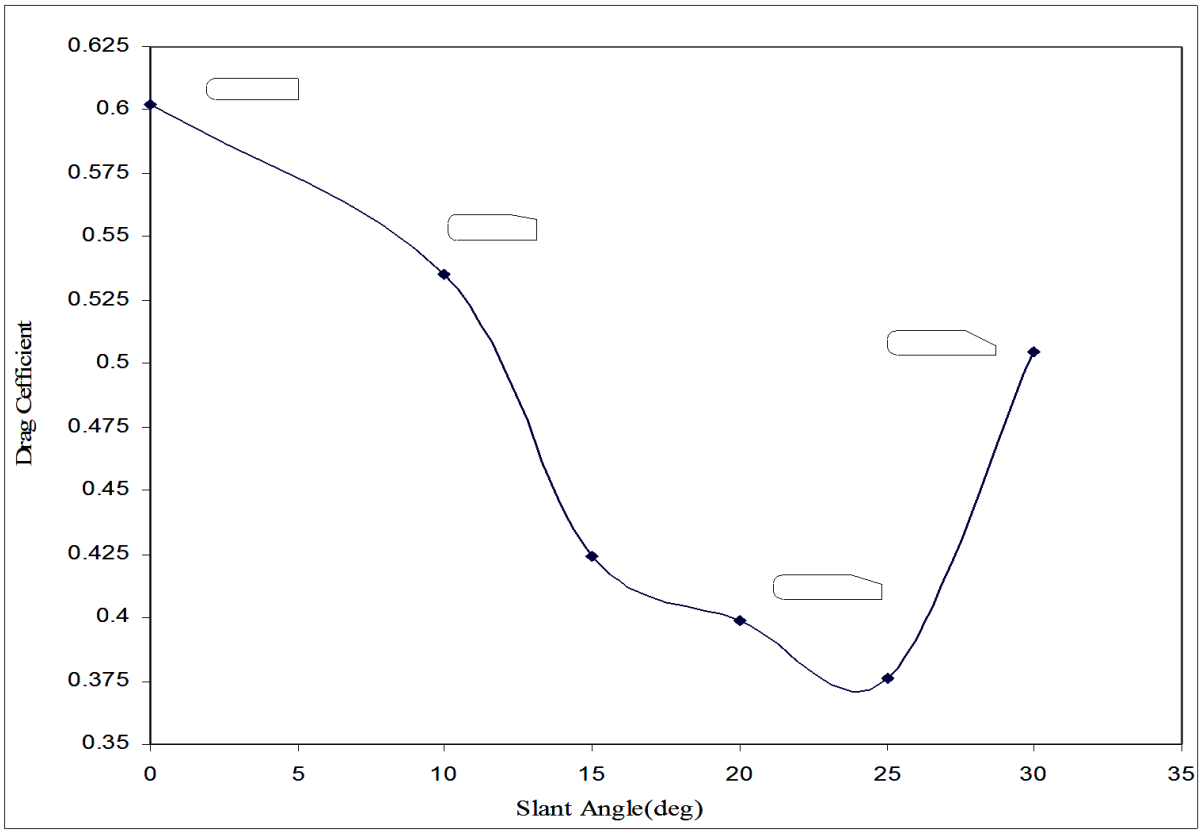

Figure 3: *Effect of slant angle on drag coefficient for Ahmed body at constant Reynolds number (Re= 28.59 x 105)*

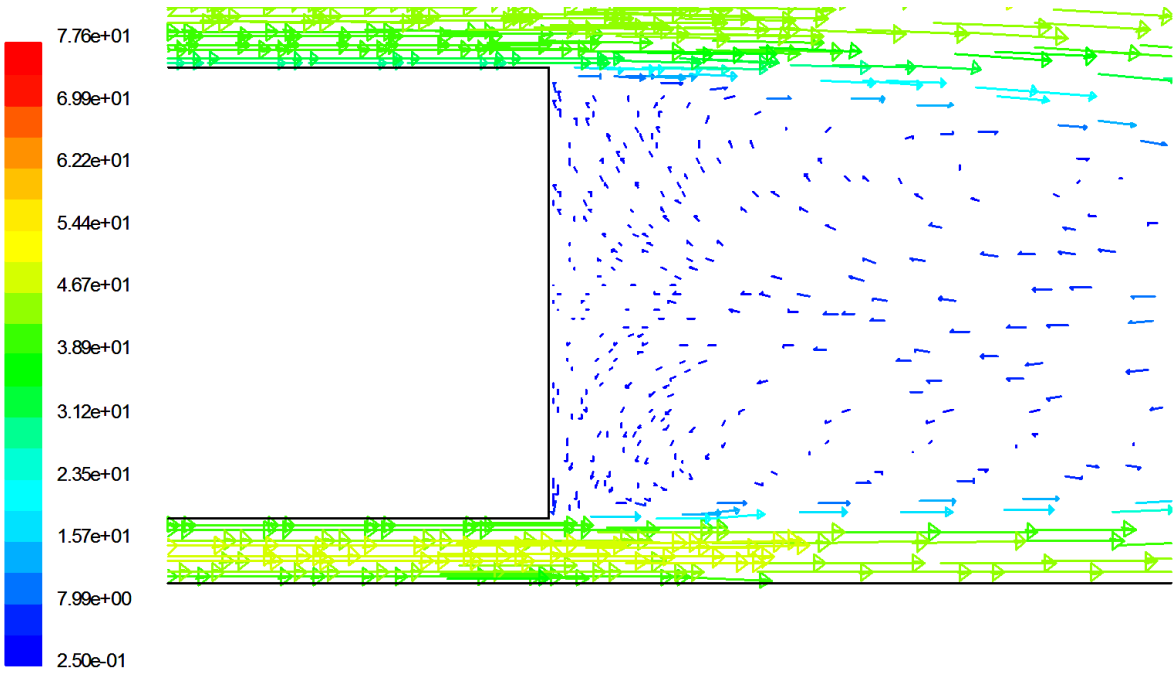

Figure 4: *Velocity vectors for Ahmed Body at 0 degree slant angle and constant Reynolds number (Re=28.59x105)*

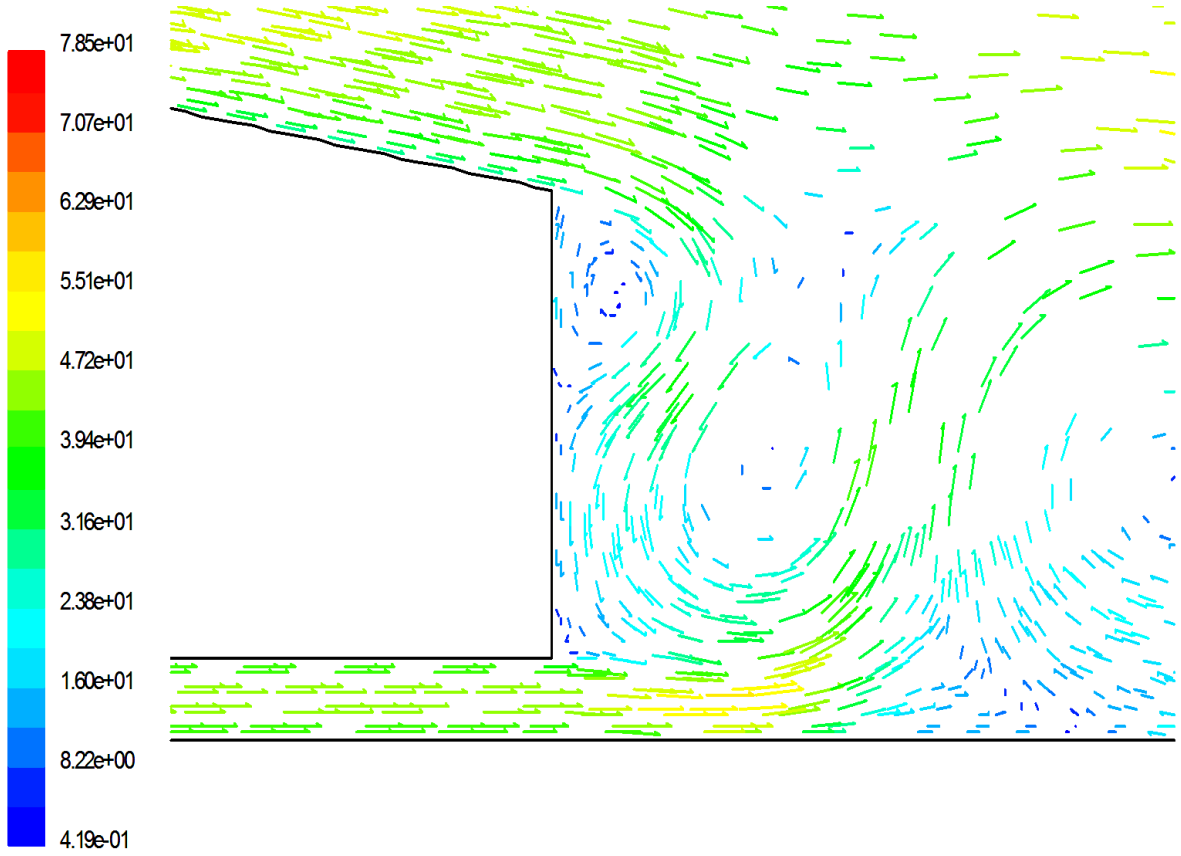

Figure 5: *Velocity vectors for Ahmed Body at 10 degree slant angle and constant Reynolds number (Re=28.59x105).*

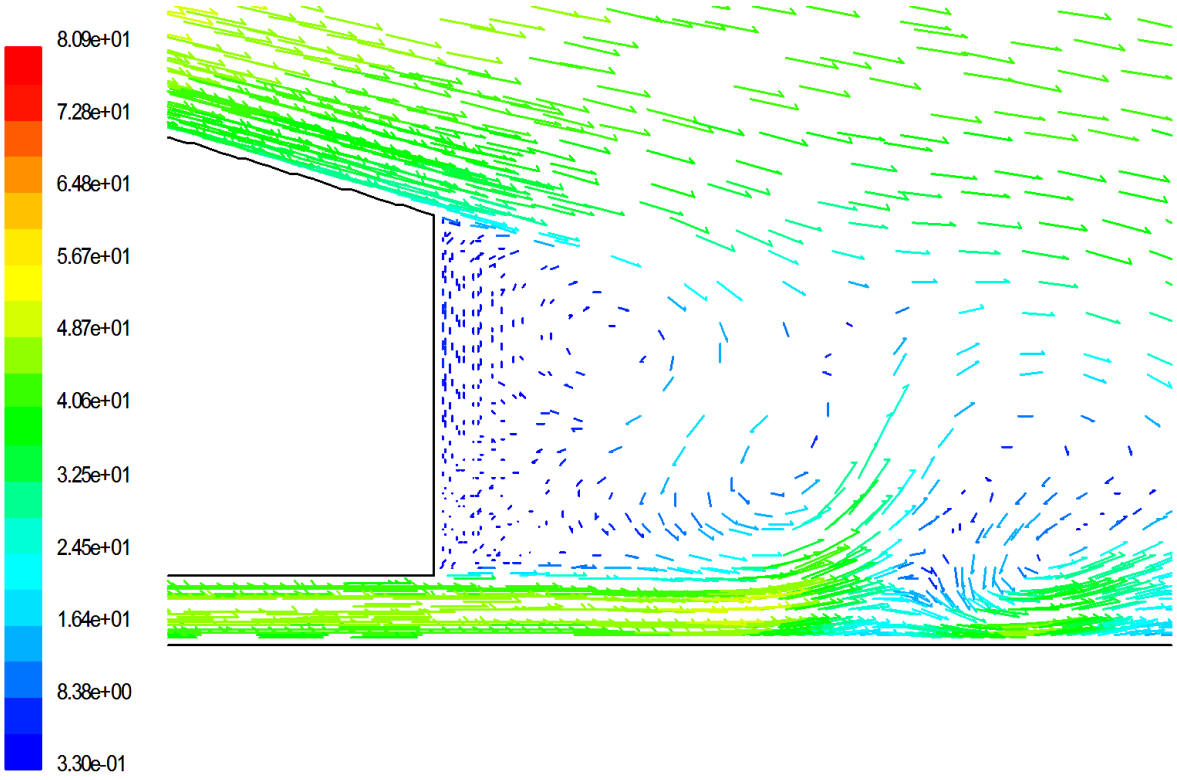

Figure 6: *Velocity vectors for Ahmed Body at 15 degree slant angle and constant Reynolds number (Re=28.59x105).*

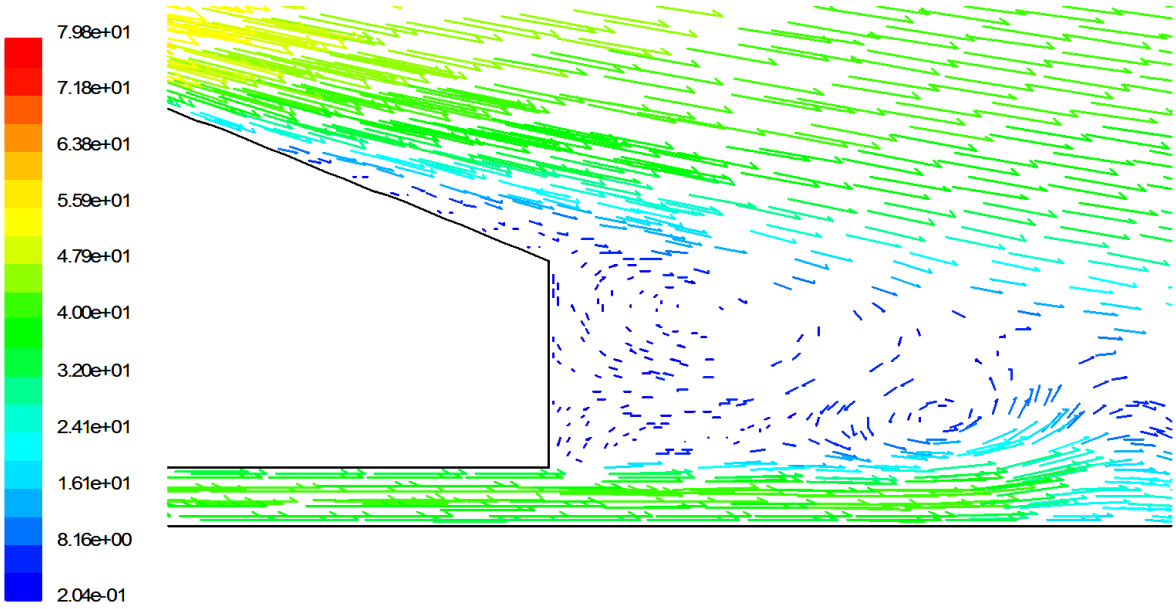

Figure 7: *Velocity vectors for Ahmed Body at 25 degree slant angle and constant Reynolds number (Re=28.59x105).*

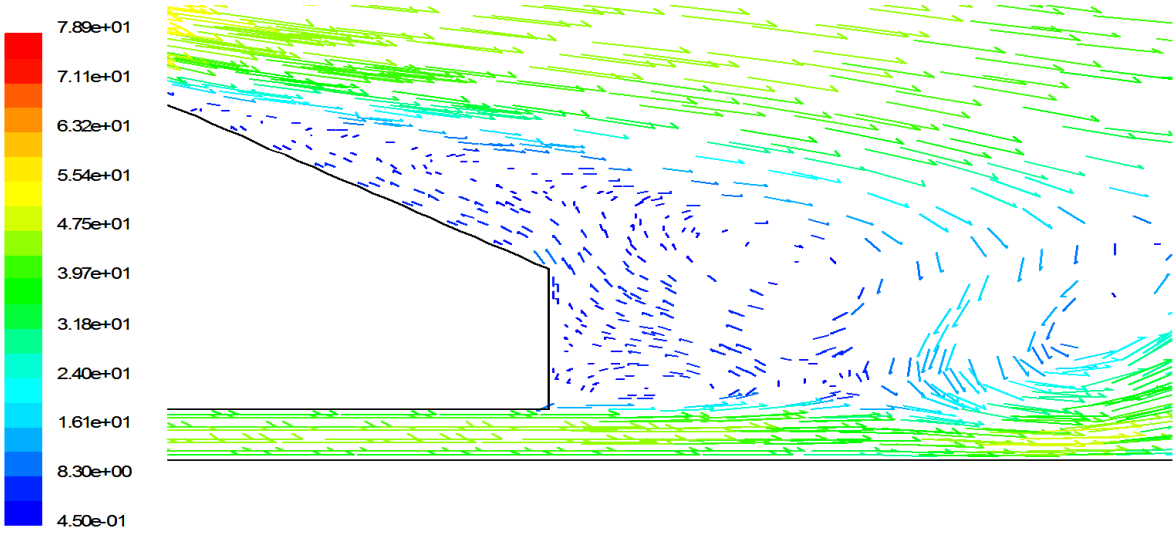

Figure 8: *Velocity vectors for Ahmed Body at 30 deg slant angle and constant Reynolds number (Re=28.59x105).*

The effect of Reynolds number on drag coefficient for different slant angles

Figure 9 shows the effect of Reynolds number on drag coefficient for 0° slant angle at different flow velocities. As Reynolds number increases from 11.913 x 105 to 19.856 x 105 corresponding to flow velocities 60 km/hr to 100 km/hr the drag coefficient decreases from 0.5964 to 0.5905, but for Re = 23.827 x 105 corresponding to 120km/hr we get the minimum drag coefficient (Cd = 0.5879). Vortices generated behind the rear end of the body are shown in Figure 10 (a, b, c, d and e). For 0 degree slant angle as Reynolds number is increased owing to decrease of viscous drag up to Re = 23.827x105 where, the viscous drag starts to increase. This is clearly demonstrated from the resemblance of the system of vortices in the whole range of Reynolds number.

Figure 11 shows the effect of Reynolds number on drag coefficient for Ahmed body at 10 degree slant angle at different

flow velocities. We observe that increasing Reynolds number from (11.913 x 105 to 19.856 x 105) corresponding to flow velocities 60 km/hr to 100 km/hr leads to increase in drag coefficient from (0.5452 to 0.6743). This is attributed to increase pressure drag, while for larger Reynolds number a large decrease in drag takes place due to delayed of separation as seen from Figure 12 (a, b, c, d and e).

Figure 13 shows the effect of Reynolds number on drag coefficient for Ahmed body at 25 degree slant angle. By increasing Reynolds number a small change in drag coefficient is observed ranging from (0.401 to 0.4204) for Reynolds number range from (11.913 x 105 to 19.856 x 105). For larger Reynolds number, (Re = 28.592 x 105) the drag coefficient decreased to reach minimum optimum value (Cd = 0.3765) corresponding to 144 km/hr flow velocity. This is due to the delayed of separation with increasing Reynolds number as can be seen from Fig. (14 a, b, c, d and e).

Figure 15 shows the effect of Reynolds number on drag coefficient for Ahmed body at 30 degree slant angle. As Reynolds number increases from (11.913 x 105 to 23.827 x 105), the drag coefficient increases from (0.4961 to 0.5208). This may be attributed to the early occurrence of separation as Reynolds number is increased up to Re=23.827x105 as it can be seen from Figure 16 (a, b, c, d and e).

The results for different slant angles are collected in Figure 17 for comparison of drag coefficient at different Reynolds number. For slant angle 25 degree, the minimum drag coefficient is obtained over the whole range of Reynolds number.

Figure 18 shows the effect of slant angle on drag coefficient for qualitative agreement.
Figure 19 shows the effect of slant angle on drag coefficient for experimental 3-D, computed 3-D results for Ahmed body.

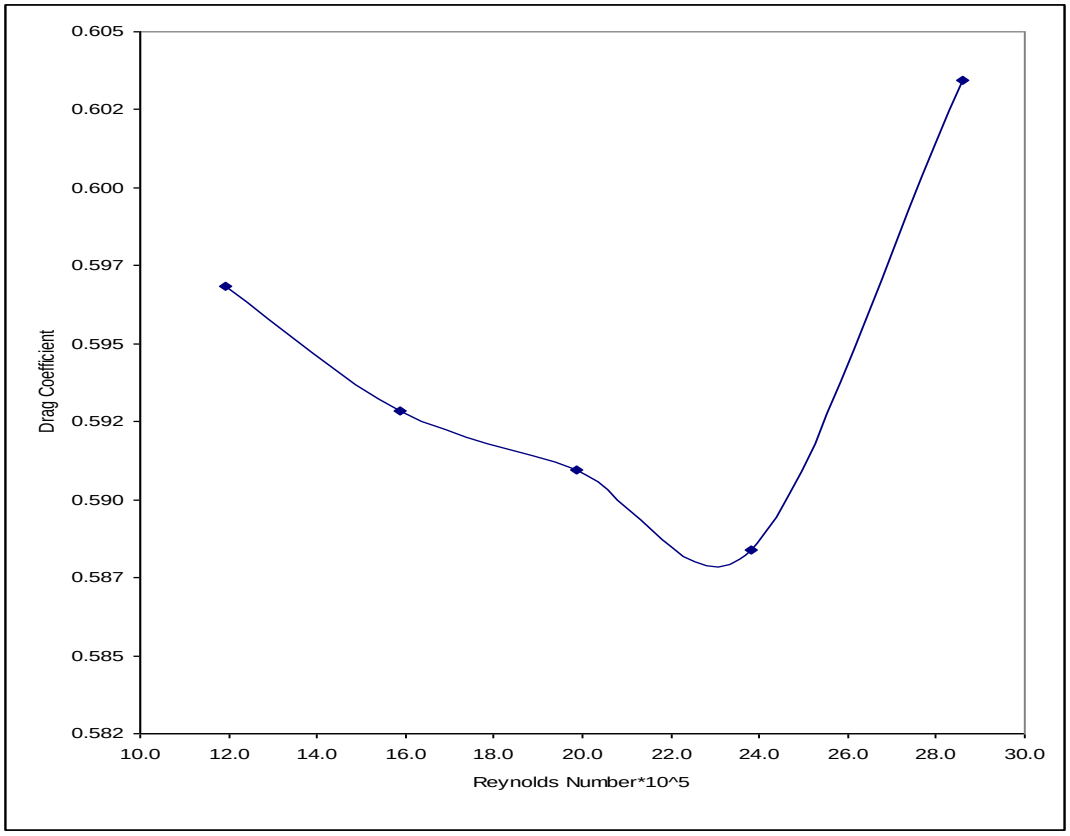

Figure 9: *Effect of Reynolds number on drag coefficient Ahmed body at 0 degree slant angle.*

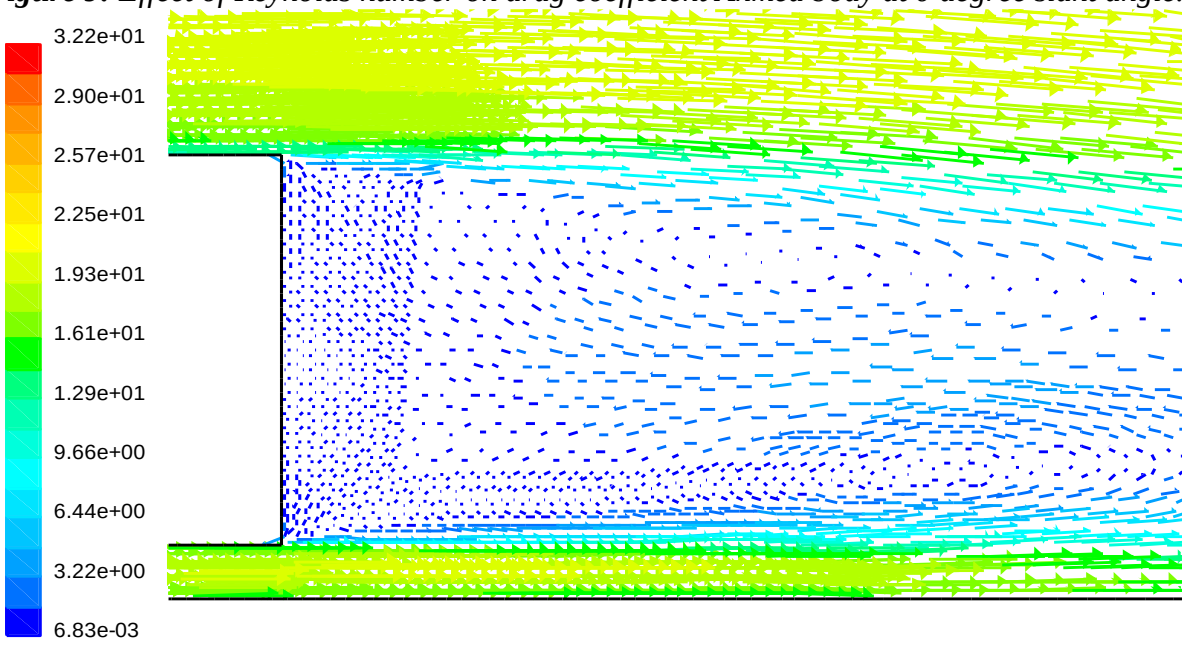

(a)

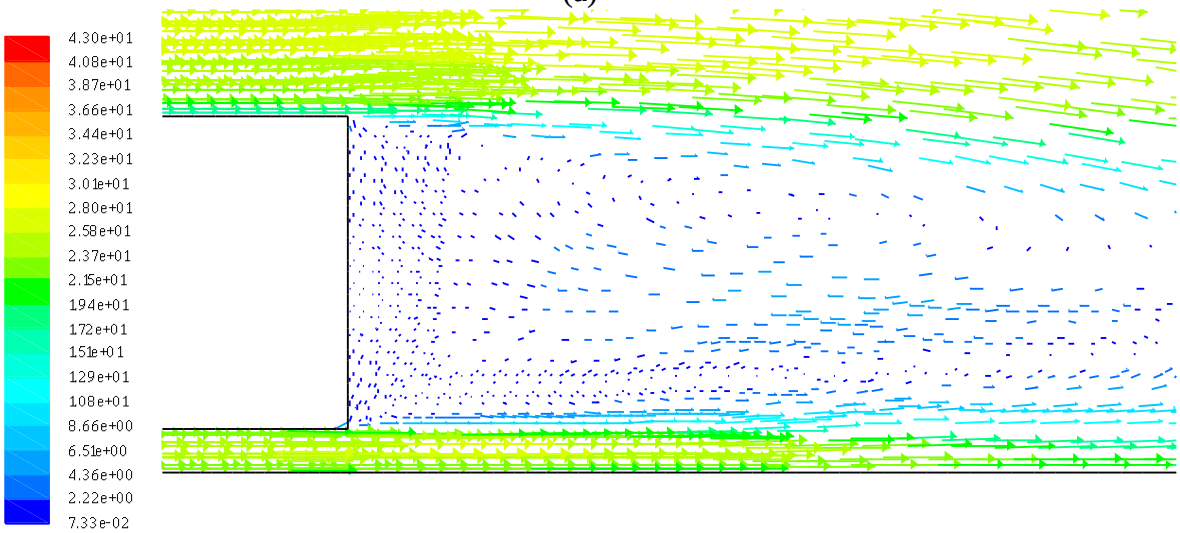

(b)

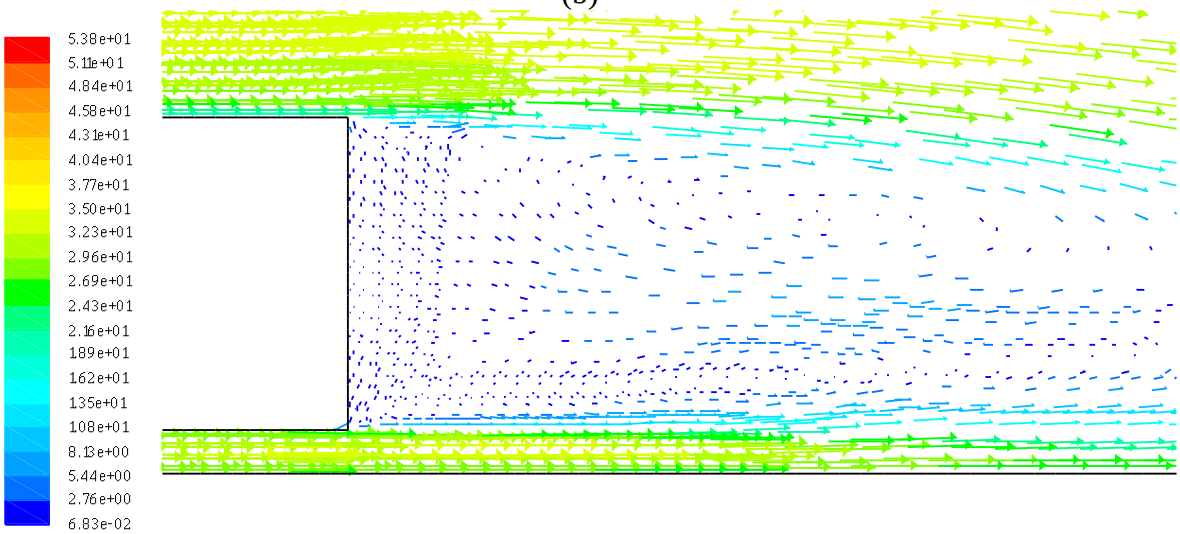

(c)

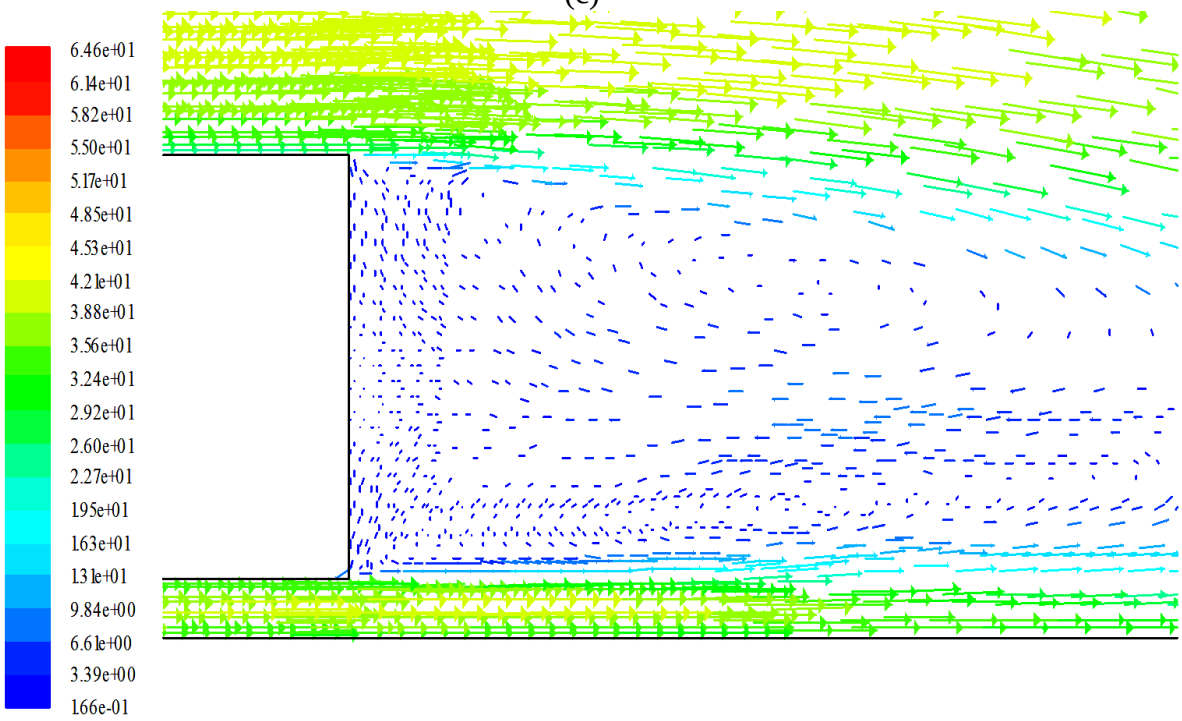

(d)

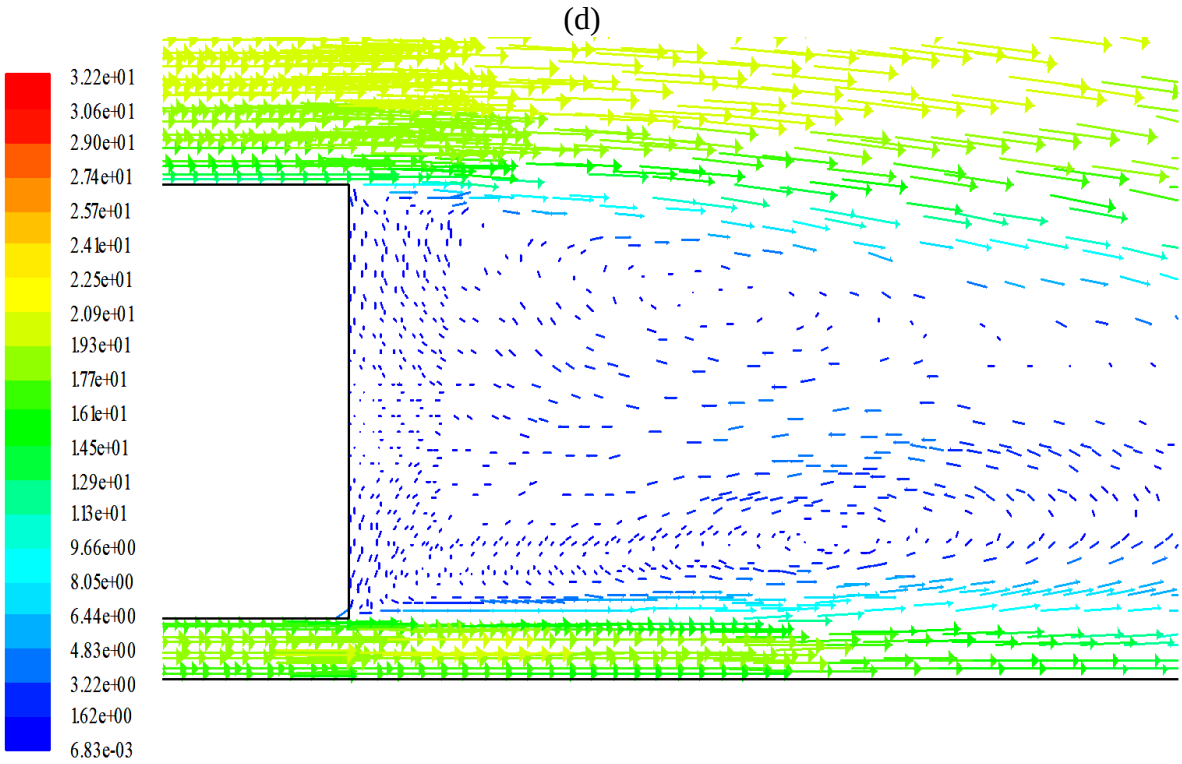

(e)

Figure 10: *Velocity vectors for Ahmed Body at 0 degree slant angle.*

a-For (Re=11.913 x105, Cd=0.5964)
b-For (Re=15.884x105, Cd=0.5923)
c-For (Re=19.856x105, Cd=0.5905)
d-For (Re=23.827x105, Cd=0.5879)

e- For (Re=28.592 x105, Cd=0.6029)

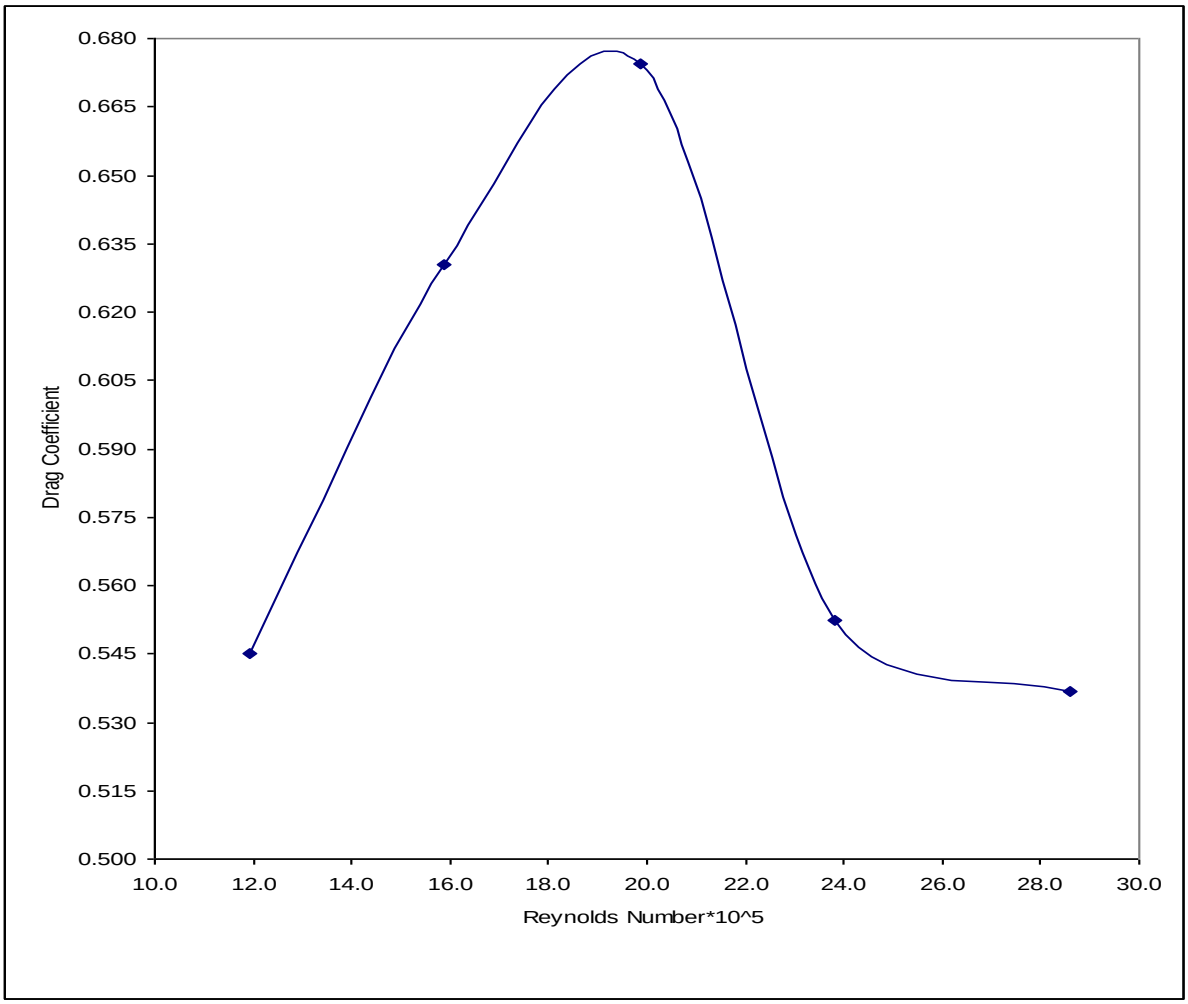

Figure 11: *Effect of Reynolds number on drag coefficient for Ahmed body at 10 degree slant angle.*

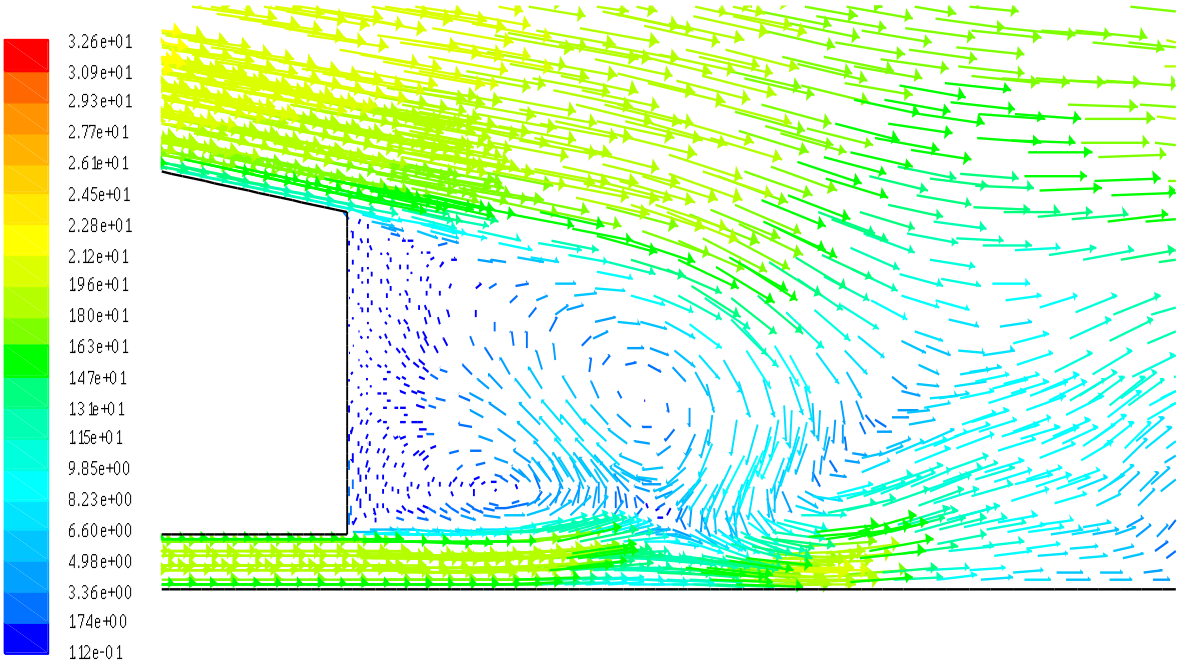

(a)

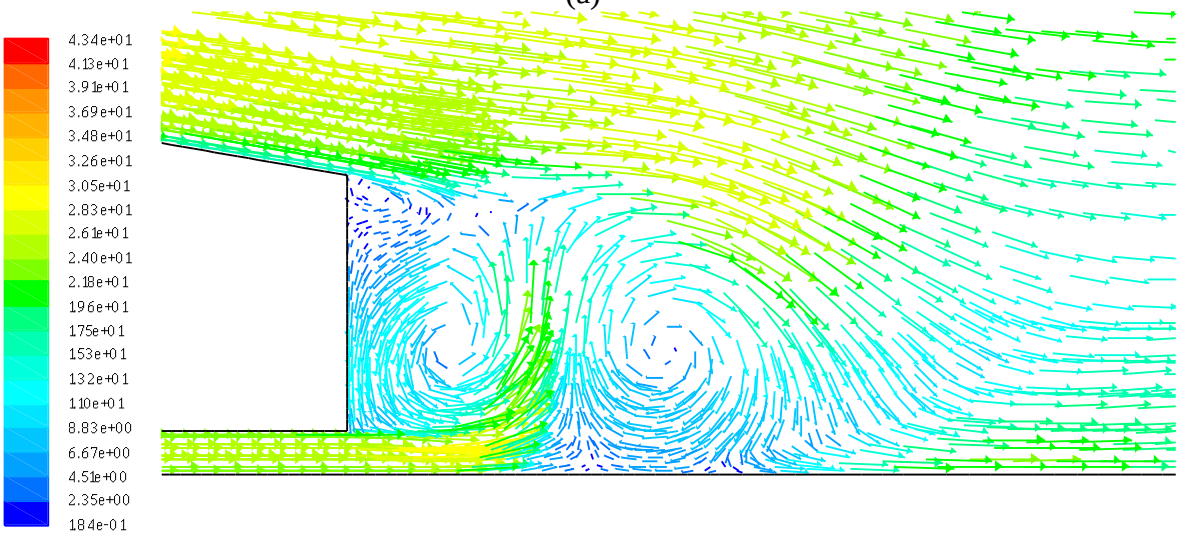

(b)

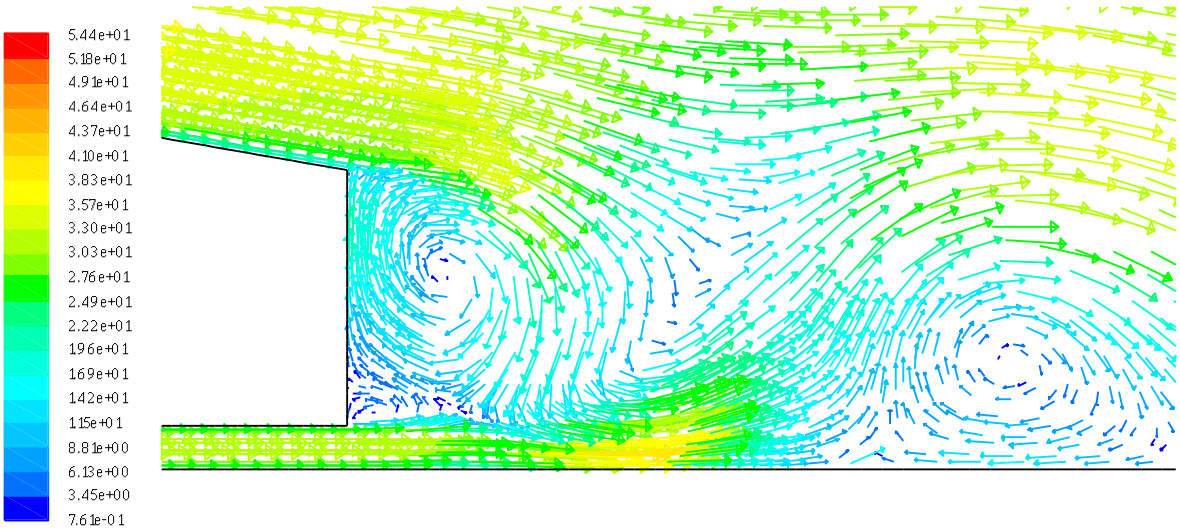

(c)

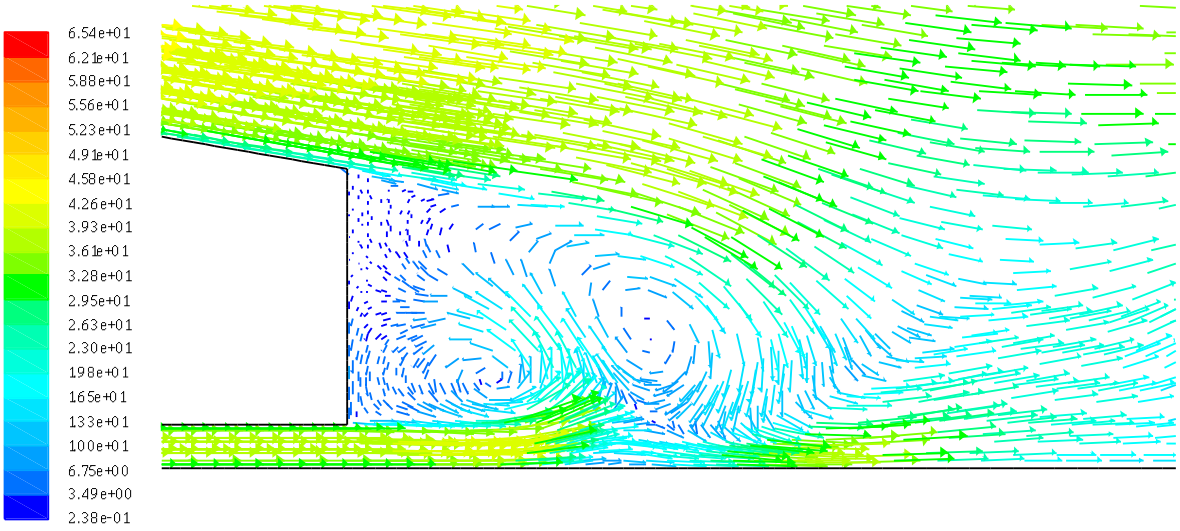

(d)

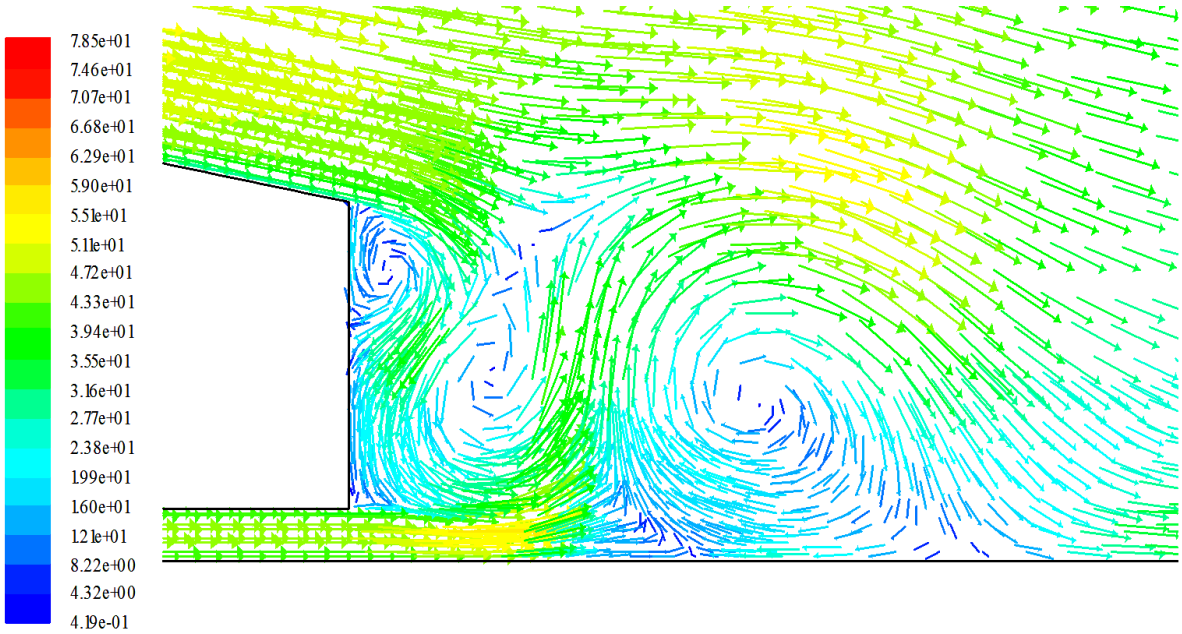

(e)

Figure 12: *Velocity vectors for Ahmed Body at 10 degree slant angle.*

a- For (Re=11.913x105, Cd=0.5452)
b- For (Re=15.884x105, Cd=0.6305)
c- For (Re=19.856 x105, Cd=0.6743)
d-For (Re=23.827 x105, Cd=0.5523)
e-For (Re=28.592 x105, Cd=0.5368)

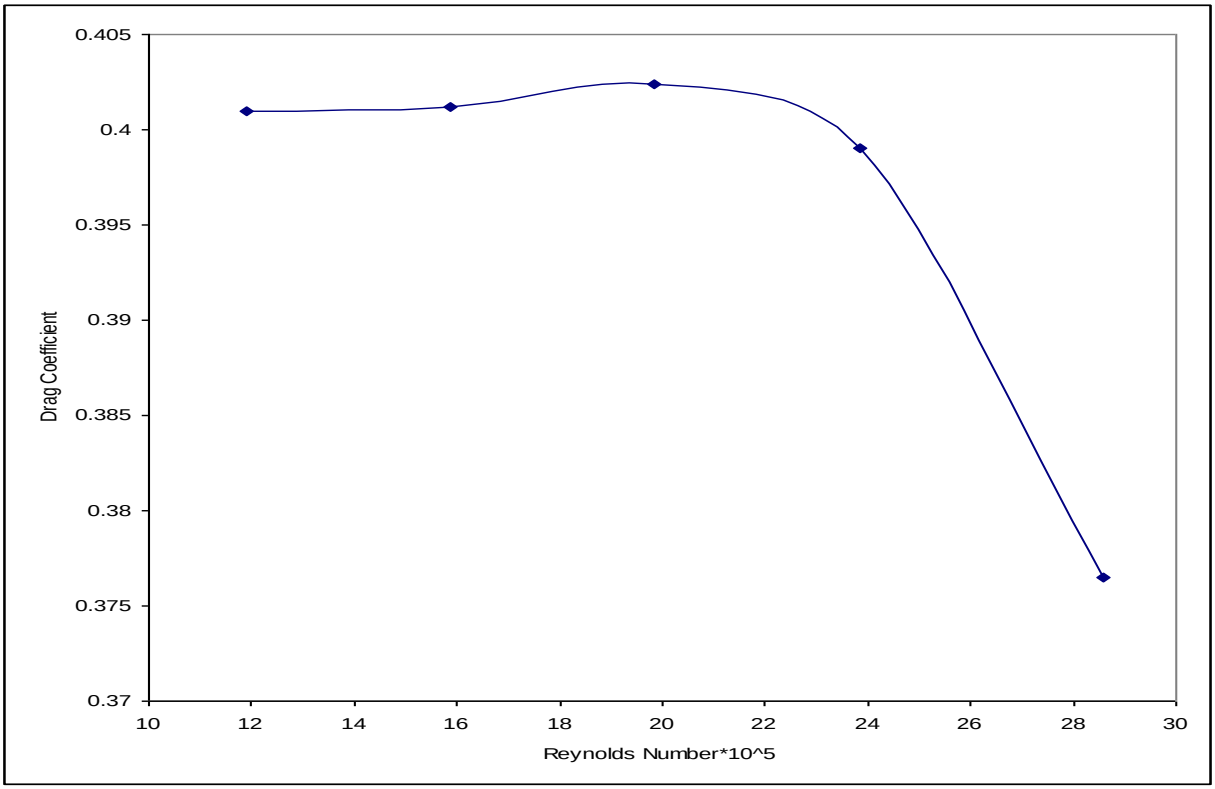

Figure 13: *Effect of Reynolds number on drag coefficient for Ahmed body at 25 degree slant angle.*

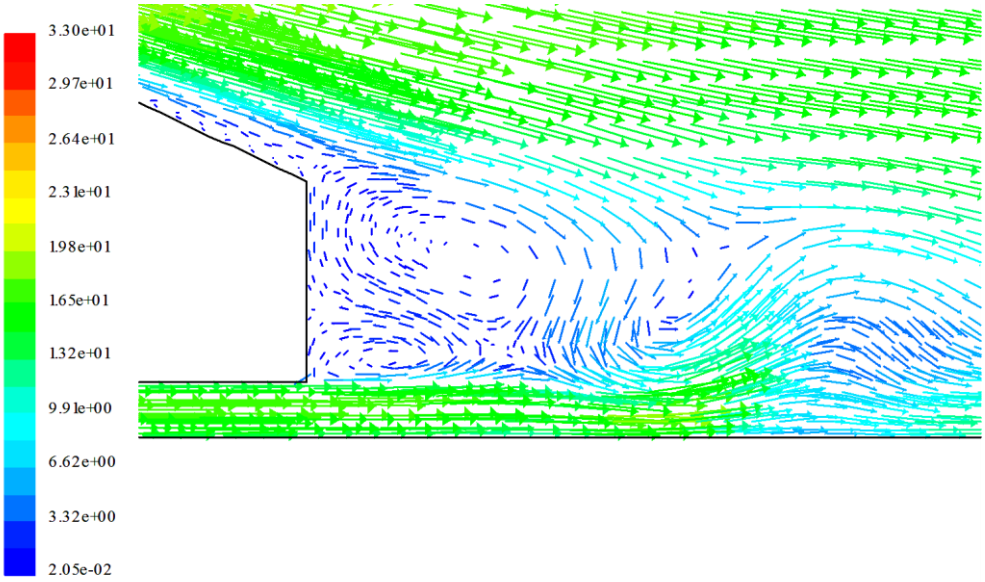

(a)

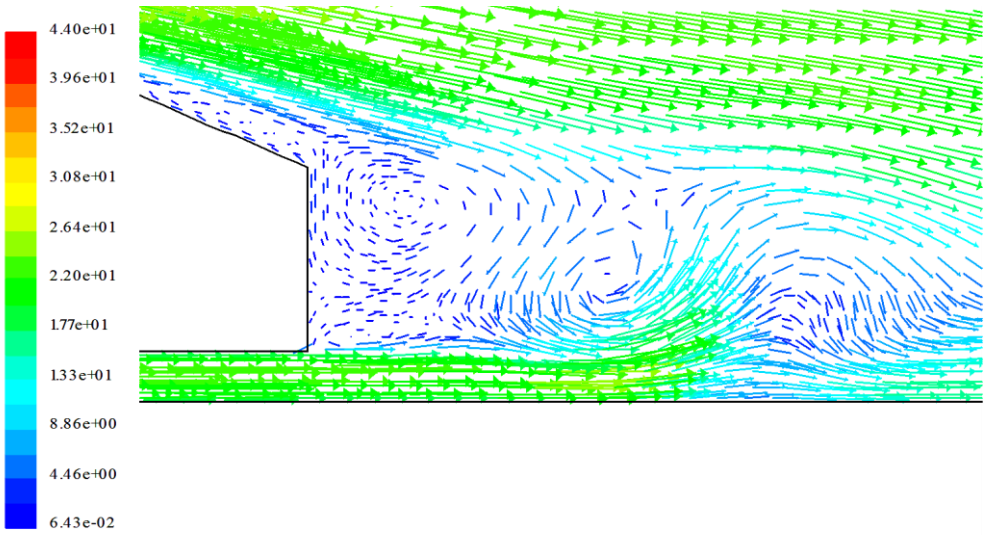

(b)

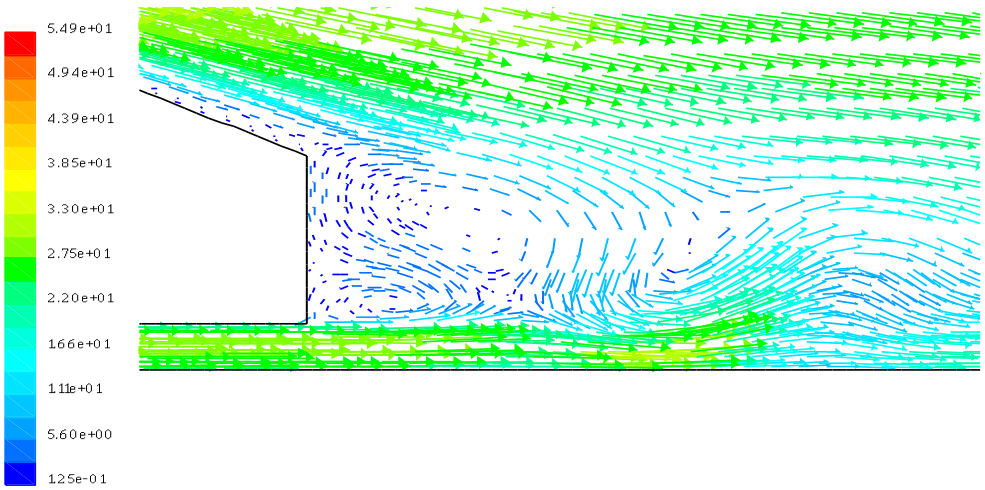

(c)

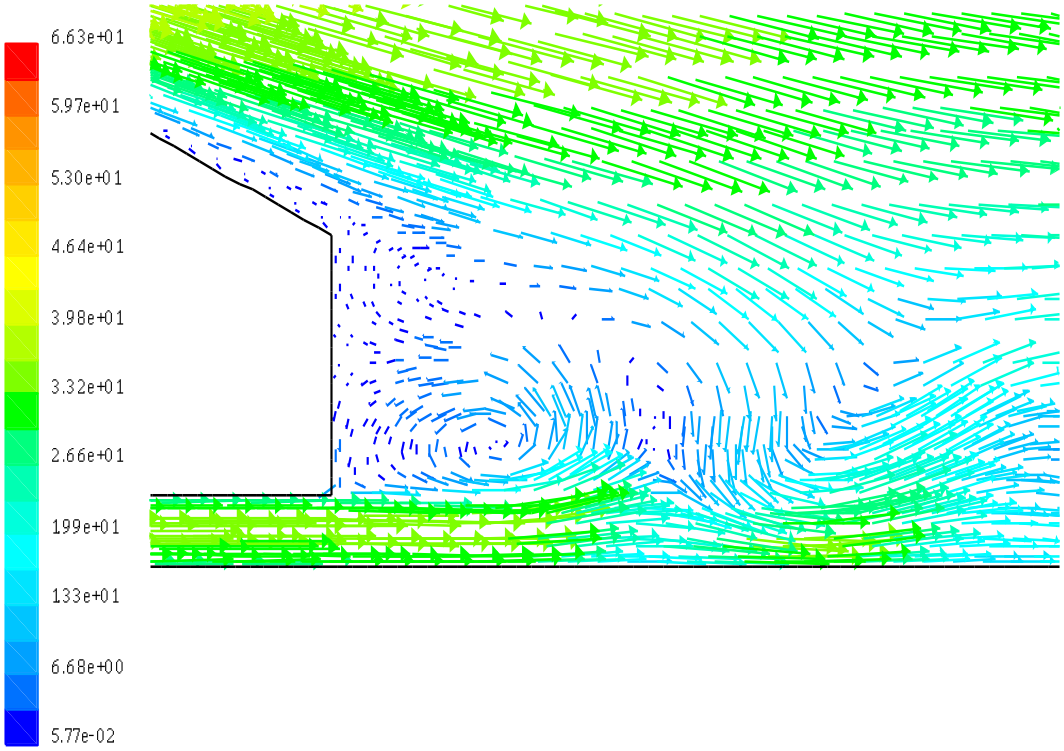

(d)

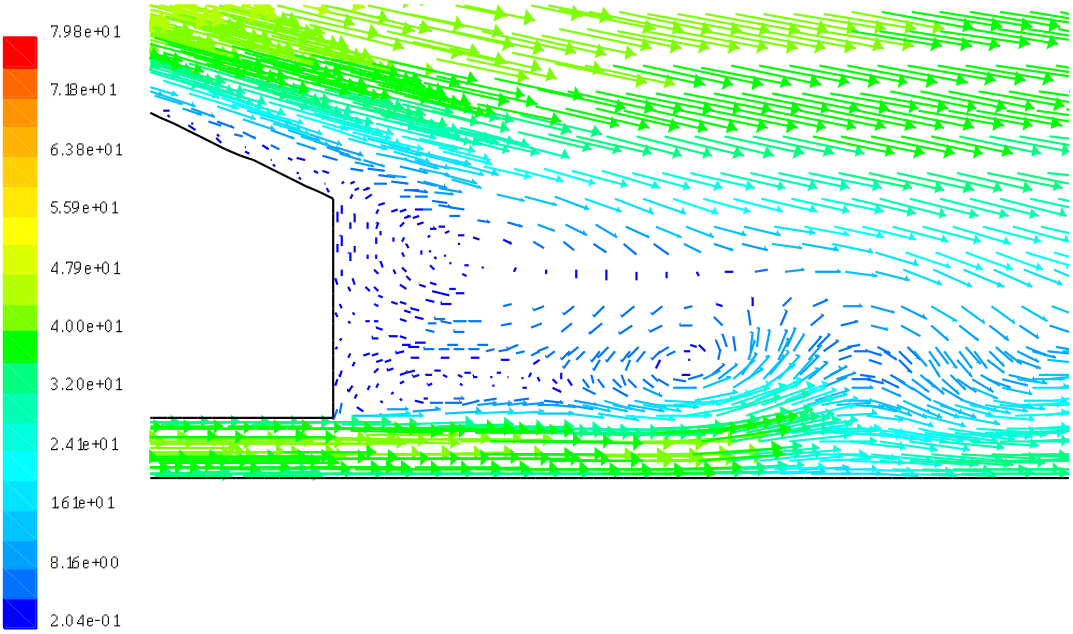

(e)

Figure 14: *Velocity vectors for Ahmed Body at 25 degree slant angle.*

a- For (Re=11.913x105, Cd=0.4010)
b- For (Re=15.884x105, Cd=0.4012)
c- For (Re=19.856 x105, Cd=0.4024)
d-For (Re=23.827 x105, Cd=0.3993)
e-For (Re=28.592 x105, Cd=0.3765)

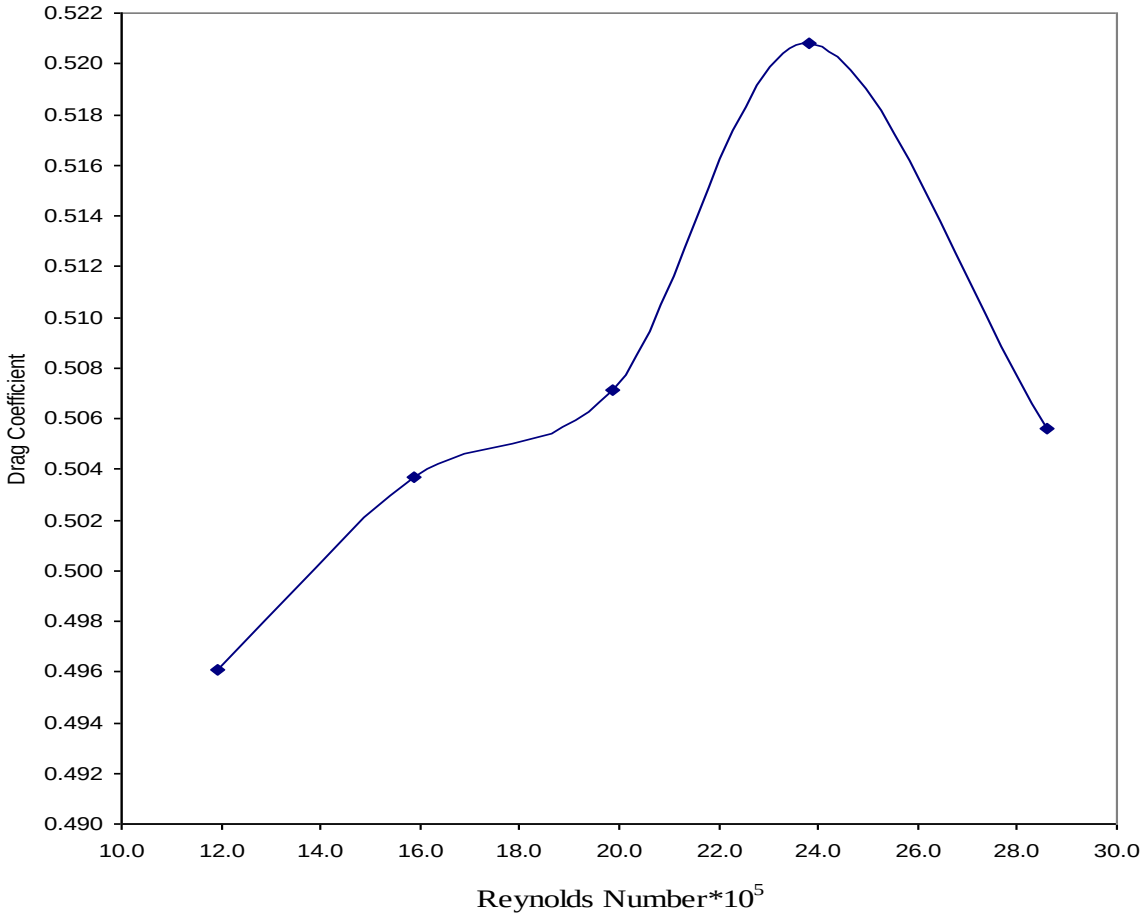

Figure 5.14 Effect of Reynolds number on drag coefficient
for ahmed body at 30 deg slant angle(appendix 5)

Figure 15: *Effect of Reynolds number on drag coefficient for Ahmed body at 30 degree slant angles.*

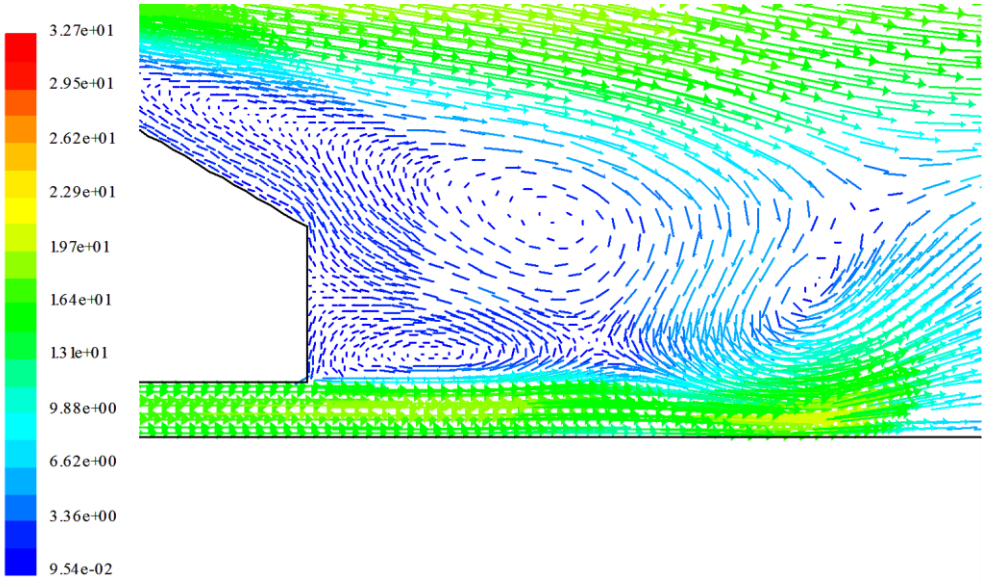

(a)

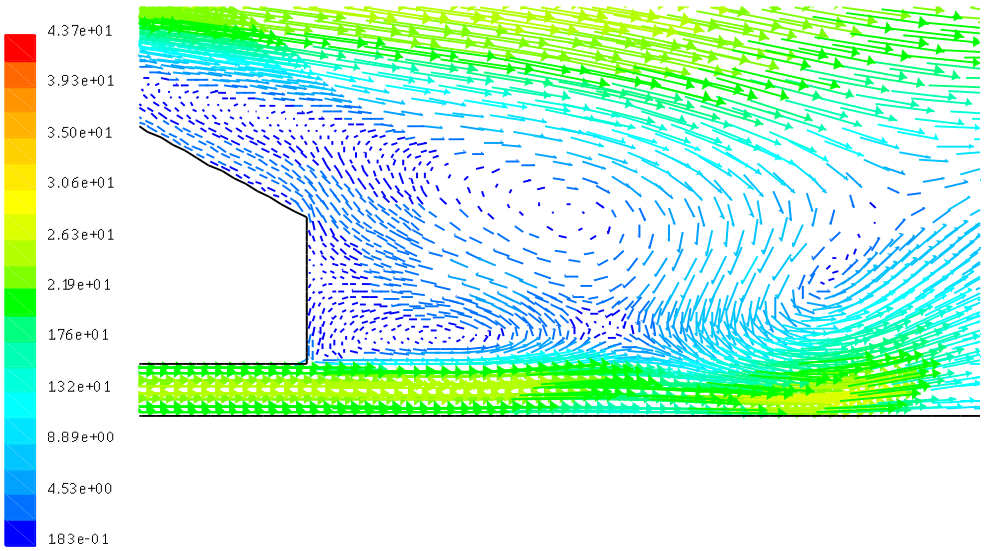

(b)

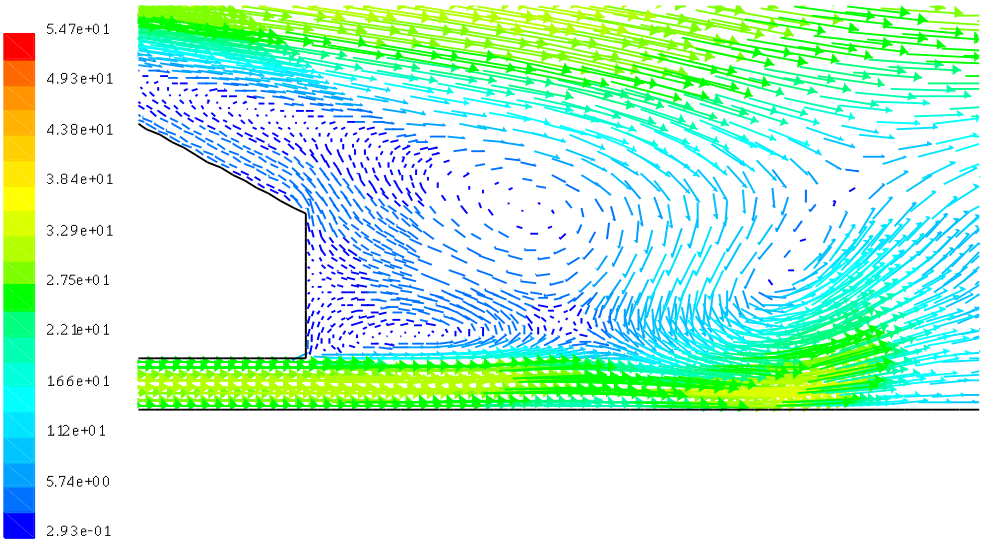

(c)

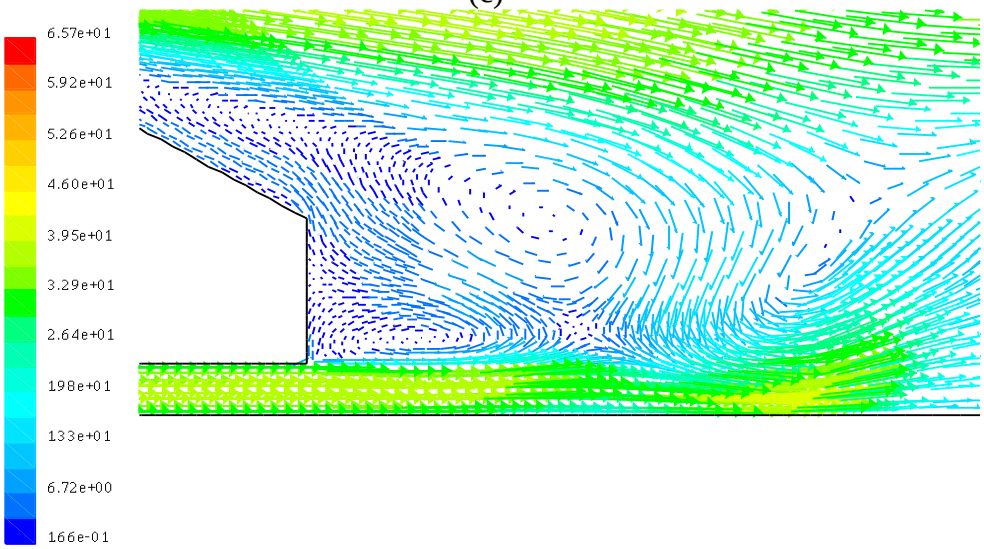

(d)

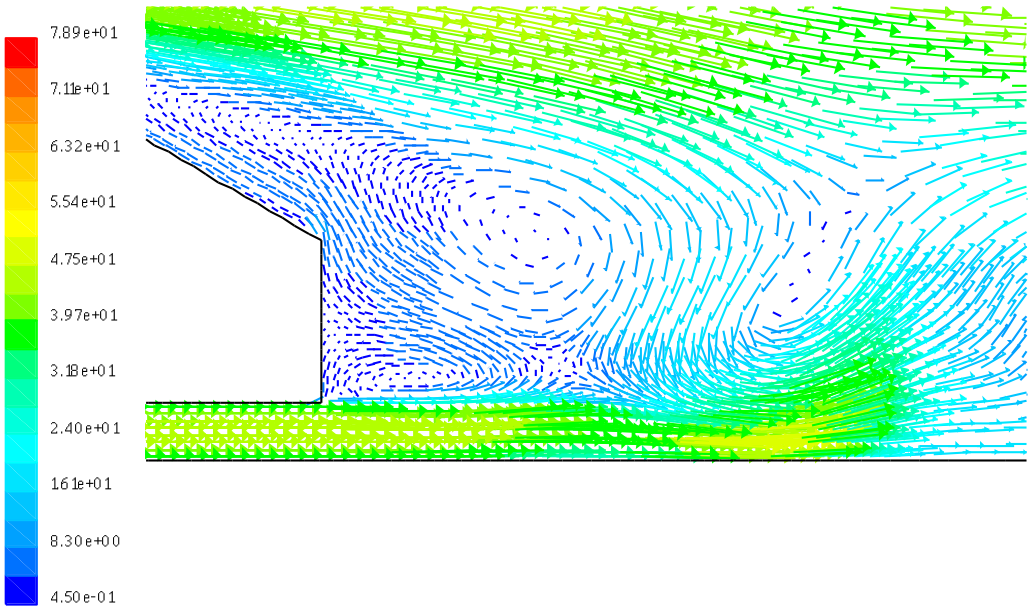

(e)

Figure 16: *Velocity vectors for Ahmed Body at 30 degree slant angle.*

a- For (Re=11.913x105, Cd=0.4961)
b- For (Re=15.884x105, Cd=0.5037)
c- For (Re=19.856 x105, Cd=0.5071)
d-For (Re=23.827 x105, Cd=0.5208)
e-For (Re=28.592 x105, Cd=0.5056)

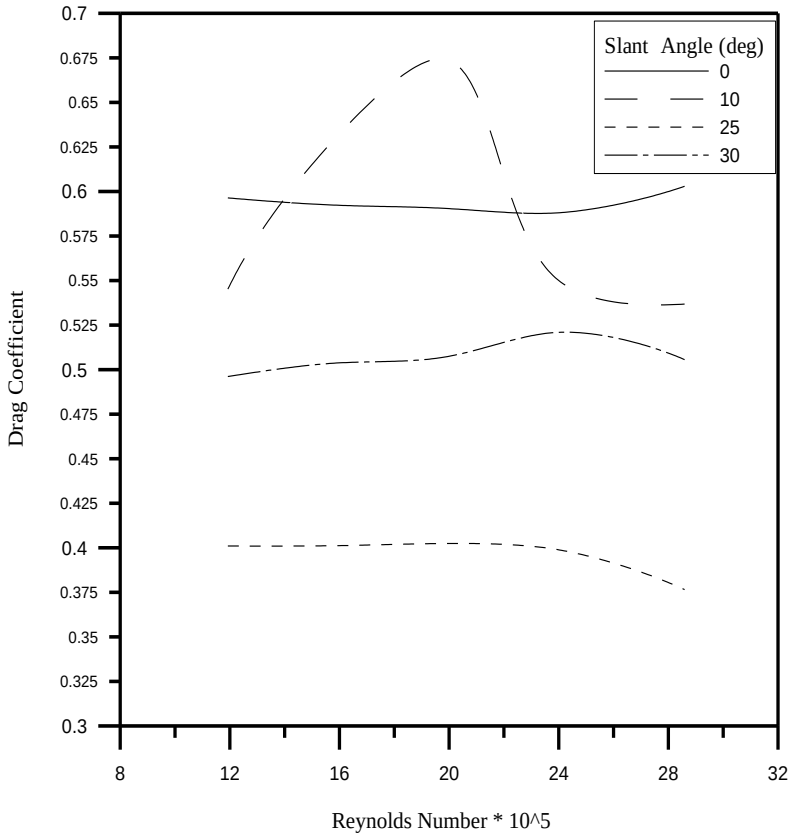

Figure 17: *Effect of Reynolds number on drag coefficient for Ahmed body at different slant angles.*

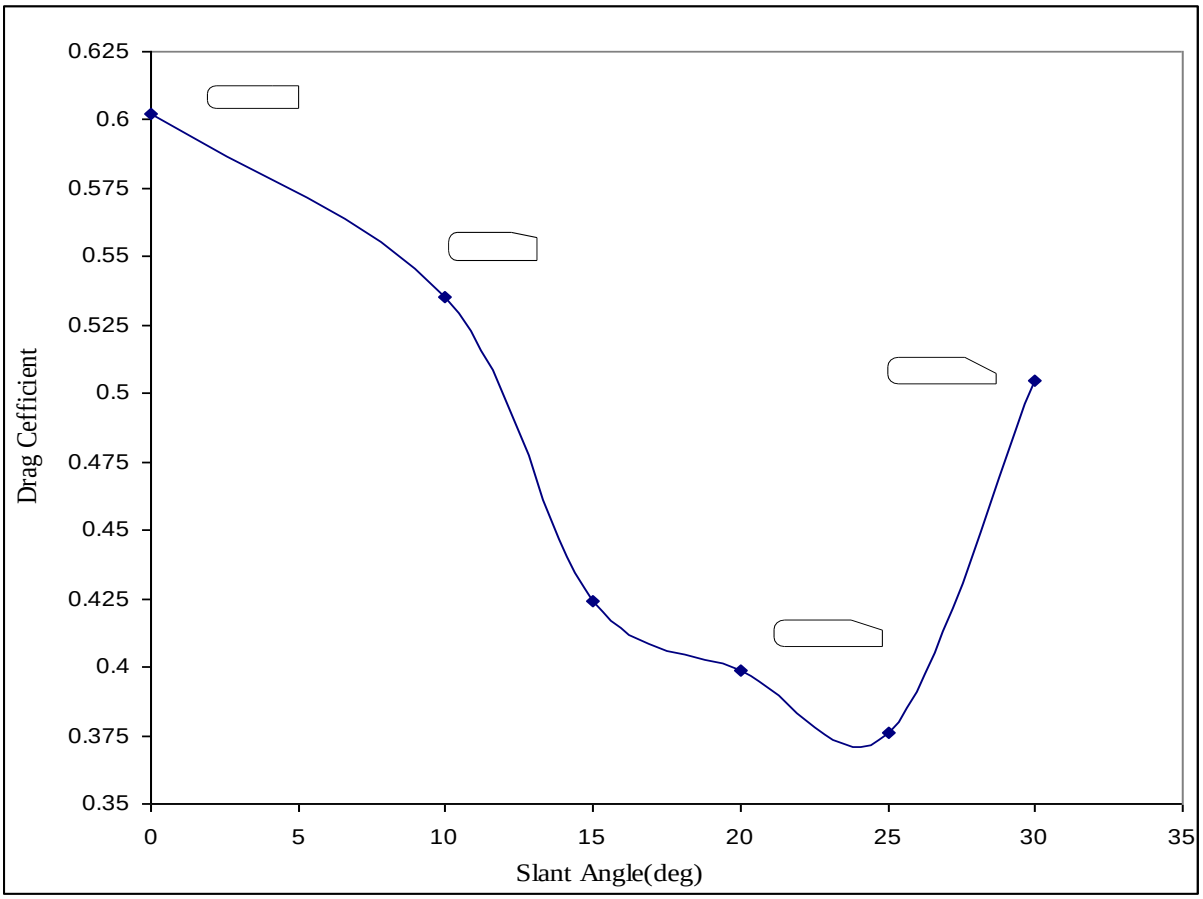

Figure 18: *Effect of slant angle on drag coefficient for qualitative agreement.*

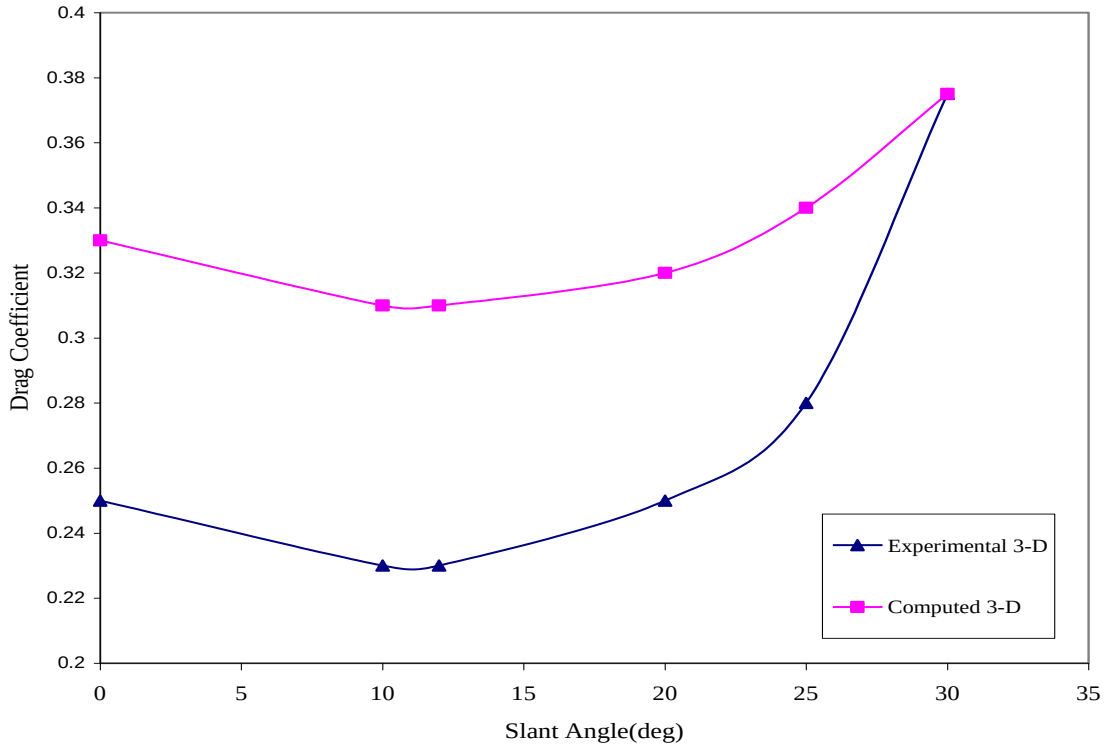

Figure 19: *Effect of slant angle on drag coefficient for experimental 3-D, computed 3-D results for Ahmed body (Re=28.59x105).*

CONCLUSIONS

As the rear slant angle increases, we observe a decrease in drag coefficient until we reach the 23.5° slant angle which is a critical angle results in the minimum drag coefficient C_d =0.37. For steeper slant angles >◌ 30^o, the flow over the rear slant become fully-separated and the drag coefficient increased to 0.505. For Ahmed body, it is found that a slant angle of 25^0 gives minimum vortices formation irrespective of car speed and drag coefficient equals to 0.376 which is near the minimum value of $C_{d.}$

REFERENCES

1. Ahmed S.R (1983), "Influence of base slant on the wake structure and drag of road vehicles". *Transactions of the ASME, Journal of Fluids Engineering.* Volume 105, pp. 429−434,.
2. Cobalt," Detached eddy simulation over a reference Ahmed car model", Aerospace sciences meeting and exhibit, Nevada, 2003.
3. Gillieron, P, chometon F. (1999), "Modeling of stationary three dimensional separated air flows around an Ahmed reference model". *ESAIM: Proceedings,* Volume 7(www.edpsciences.org).
4. Howard, R.J.A, Pourquiue, M. (2002), "Large eddy simulation of an Ahmed reference model". *Journal of turbulence,* Volume 3.
5. Howard R.JA, Bieder U, Lesieur M (2001), "Structured and non-structured large eddy simulation of the Ahmed reference model" .In R. Friedrich, editor, proc.2001 Euromech colloquim, Munich, Derdrecht Kluwer,.
6. Chauhan Rajsinh B. et al (30th March 2012), "Numerical investigation of external flow around the Ahmed reference body using computational fluid dynamics". *School of Mechanical and Building Sciences, VIT University, Vellore.*
7. Hugo G, et al (19−22 November 2013, "Computational study of unsteady road vehicle aerodynamics including fluid-structure interaction" *Mecánica Computacional,* Volume XXXII, pp. 1409-1425 (artículo completo) Carlos G. García Garino, Aníbal E. Mirasso, Mario A. Storti, Miguel E. Tornello (Eds.) Mendoza, Argentina,.
8. Deepak K. et al (May 2013), "Computational Study of Flow around a Simplified 2-D Ahmed Body" *International Journal of Engineering Science and Innovative Technology (IJESIT),* Volume 2, Issue 3.
9. Patil, S., Woodiga, Ahn, H (2015), "Fluid Structure Interaction Simulations Applied to Automotive Aerodynamics," *SAE Technical Paper.*
10. N Yusuke, Y Tsuyoshi, T Hiroshi, T Jiro (2015), "Analysis of unsteady aerodynamics of a car model in dynamic pitching motion using LS-DYNA" *Thirteenth International LS-DYNA,*.